

Chitosan – poly(butylene succinate) scaffolds and human bone marrow stromal cells induce bone repair in a mouse calvaria model

A. R. Costa-Pinto^{1,2*}, V. M. Correlo^{1,2}, P. C. Sol^{1,2}, M. Bhattacharya³, S. Srouji^{4,5}, E. Livne⁴, R. L. Reis^{1,2} and N. M. Neves^{1,2}

¹3Bs Research Group – Biomaterials, Biodegradables and Biomimetics, Department of Polymer Engineering, Headquarters of the European Institute of Excellence on Tissue Engineering and Regenerative Medicine University of Minho, Avepark, S. Cláudio do Barco, 4806-909 Caldas das Taipas, Guimarães, Portugal

²Institute for Biotechnology and Bioengineering (IBB), PT Government Associated Laboratory, Guimarães, Portugal

³Department of Biosystems Engineering, University of Minnesota, St Paul, MN 55108, USA

⁴Anatomy and Cell Biology, Faculty of Medicine, Technion-IIT, Haifa 32000, Israel

⁵Oral and Maxillofacial Surgery Department, Carmel Medical Centre, Haifa 34354, Israel

Abstract

Tissue engineering sustains the need of a three-dimensional (3D) scaffold to promote the regeneration of tissues in volume. Usually, scaffolds are seeded with an adequate cell population, allowing their growth and maturation upon implantation *in vivo*. Previous studies obtained by our group evidenced significant growth patterns and osteogenic differentiation of human bone marrow mesenchymal stem cells (hBMSCs) when seeded and cultured on melt-based porous chitosan fibre mesh scaffolds (cell constructs). Therefore, it is crucial to test the *in vivo* performance of these *in vitro* 3D cell constructs. In this study, chitosan-based scaffolds were seeded and cultured *in vitro* with hBMSCs for 3 weeks under osteogenic stimulation conditions and analysed for cell adhesion, proliferation and differentiation. Implantation of 2 weeks precultured cell constructs in osteogenic culture conditions was performed into critical cranial size defects in nude mice. The objective of this study was to verify the scaffold integration and new bone formation. At 8 weeks of implantation, scaffolds were harvested and prepared for micro-computed tomography (μ CT) analysis. Retrieved implants showed good integration with the surrounding tissue and significant bone formation, more evident for the scaffolds cultured and implanted with human cells. The results of this work demonstrated that chitosan-based scaffolds, besides supporting *in vitro* proliferation and osteogenic differentiation of hBMSCs, induced bone formation *in vivo*. Thus, their osteogenic potential in orthotopic location in immunodeficient mice was validated, evidencing good prospects for their use in bone tissue-engineering therapies. Copyright © 2011 John Wiley & Sons, Ltd.

Received 28 October 2010; Accepted 11 November 2010

Keywords bone regeneration; chitosan; tissue engineering; bone marrow stromal cells; cranial defect; nude mice

1. Introduction

Tissue engineering has emerged in the last 17 years as a new regenerative approach for the treatment of a variety of tissues, including bone. The concept is based on the development of strategies aimed at obtaining tissue and organ equivalents that can replace or restore the natural features and physiological functions of natural tissues

*Correspondence to: A. R. Costa-Pinto, 3Bs Research Group – Biomaterials, Biodegradables and Biomimetics, University of Minho, Headquarters of the European Institute of Excellence on Tissue Engineering and Regenerative Medicine, AvePark, Zona Industrial da Gandra, S. Cláudio do Barco, 4806-909 Caldas das Taipas, Guimarães, Portugal
E-mail: arpinto@dep.uminho.pt

in vivo (Langer and Vacanti, 1993). One of the fundamental principles relies on the need of a specific cell population in combination with a 3D structure, in order to promote, in volume, tissue regeneration (Hutmacher *et al.*, 2007).

The ideal cell population is considered to be autologous undifferentiated stem cells that can be isolated from adult sources. Although embryonic stem cells display an enormous potential, they raise ethical and moral issues, mainly because of the removal and destruction of human embryos (Hipp and Atala, 2008). In this context, adult stem cells present an alternative option, being isolated from several sources, such as bone marrow (Bianco and Robey, 2001), brain, liver, skin, skeletal muscle, intestine, pancreas, peripheral blood, dental pulp (Hipp and Atala, 2008), adipose tissue (Gimble and Guilak, 2003) or fetal tissues such as umbilical cord (Sarugaser *et al.*, 2005) or amniotic fluid. Stem cells are defined as cells that have clonogenic and self-renewing capabilities and that differentiate into multiple cell lineages (Weissman, 2000).

Mesenchymal stem cells (MSCs) can be combined with appropriate carriers (scaffolds) where a cell population will be grown and further implanted *in vivo*. Scaffolds used for tissue-engineering purposes mimic the extracellular matrix (ECM) of the regenerating bone environment. Selection of the material for scaffold production in bone-related applications is a very important step towards the creation of a tissue-engineered construct (Martins *et al.*, 2009).

In recent years, natural polymers emerged as an alternative to synthetic polymers, mainly due to their biocompatibility and biodegradability. Most of the synthetic biomaterials are effective in supporting bone regeneration, either alone or in conjunction with growth factors, although they display limitations. Ideally this structure should be biodegradable, allowing cells to adhere and proliferate, leading to the formation of ECM (Salgado *et al.*, 2004). Different naturally based polymers have been proposed for this demanding application, such as starch (Gomes *et al.*, 2001; Salgado *et al.*, 2002) and chitosan (Costa-Pinto *et al.*, 2008, 2009; Malafaya *et al.*, 2005; Martins *et al.*, 2008). Chitosan has shown an excellent combination of properties, including non-antigenicity and non-cytotoxicity, making this biomaterial quite attractive for bone tissue-engineering applications (Di Martino *et al.*, 2005; Zarzycki and Modrzejewska, 2003).

We have developed a set of biomaterials using the thermal-based processing of thermoplastic polymers, by blending chitosan (Ch) with different aliphatic polyesters, such as poly(caprolactone) (PCL), poly(butylene succinate) (PBS), poly(butylene terephthalate adipate) (PBTA) and poly(butylene succinate adipate) (PBSA) (Correlo *et al.*, 2005, 2009). After testing the eventual cytotoxicity of the developed scaffolds, the next step consisted of the biological screening of the most suitable scaffold formulation for bone tissue-engineering applications. For that, we tested several blends with a mouse mesenchymal stem cell line (BMC9), promoting differentiation into the

osteogenic lineage. The results evidenced that the chitosan–PBS blend formulation, 50% wt and 60% porosity, showed the best performance in terms of cell behaviour (Costa-Pinto *et al.*, 2008). Further studies were performed using human bone marrow mesenchymal stem cells (hBMSCs) in fibre-mesh scaffold morphology, with excellent results in terms of cell adhesion, proliferation and osteogenic differentiation (Costa-Pinto *et al.*, 2009). Also, osteogenic differentiation of these cells onto the scaffolds was consistently detected by the presence of mineralized ECM (Gupta *et al.*, 2008; Wu *et al.*, 2010). Therefore, the fibrous morphology enhanced conditions to promote cell infiltration into the inner regions of the scaffold.

Thus, the next step is to evaluate this tissue-engineering strategy *in vivo*, using a feasible animal model. For that, we have selected the cranial defect in nude mice (An and Freidman, 1998; Schmitz and Hollinger, 1986), since it enables several aspects of this strategy to be tested. The calvaria form a flat bone, which allows the creation of a uniform circular defect with an adequate size for easier surgical procedure and specimen handling. Fixation is provided by the dura mater and the overlying skin. The model has been thoroughly used and studied and is well reproduced (An and Freidman, 1998; Montjovent *et al.*, 2007; Schmitz and Hollinger, 1986). The low vascularization in cranial area turns this model into one of the toughest to evaluate the *in vivo* performance of tissue-engineered constructs (Castano-Izquierdo *et al.*, 2007). The nude mouse model is required, since human cells will be implanted, avoiding graft rejection responses from the host (Gupta *et al.*, 2008). The critical size defect (CSD) for this model is 4–5 mm. A CSD is defined as the intraosseous wound in a specific bone and species of animal without spontaneous healing during the lifetime of the animal (Wu *et al.*, 2010).

Herein, we have selected compression-moulded salt-leaching scaffolds. We considered this production method to be the most appropriate for the development of scaffolds that meet the required dimensions to fit into the animal calvaria defect. In the present study, we have assessed the *in vitro* biological behaviour of hBMSCs cultured on chitosan–PBS scaffolds, and these 3D cell constructs were validated in an *in vivo* model of a critical cranial defect in nude mice.

2. Materials and methods

2.1. Production of scaffolds

The scaffolds used in this study were produced by melt-based compression moulding followed by salt leaching. Briefly, chitosan was melt-blended with PBS (50% in weight) by extrusion and further ground into a powder. This powder was subjected to solid mixing with salt particles in the size range 250–500 µm and a salt content of 60%. Details of the processing methodology can be found elsewhere (Correlo *et al.*, 2009).

2.2. Characterization of scaffolds

Cross-sections of all the developed scaffolds were analysed using a Leica-Cambridge S-360 scanning electron microscope (SEM) for preliminary assessment on their morphology. All the samples were sputter-coated with gold prior to the SEM analysis.

To evaluate the internal 3D structure of the scaffolds, micro-computed tomography (μ CT) equipment (SkyScan, Belgium) was used as a non-destructive characterization methodology. Three scaffolds were scanned in high-resolution mode of $8.7\ \mu\text{m}$ $x/y/z$ and an exposure time of 1792 ms. The scanner energy was set to 63 keV with 157 μA current. μ CT scans followed by 3D reconstruction (μ CT analyser and a μ CT volume realistic 3D visualization, from SkyScan) of serial image sections allowed the reconstruction and analysis of the 3D microarchitecture of the scaffolds, pore morphology, determination of porosity and interconnectivity.

2.3. *In vitro* cell culture

Human bone marrow mesenchymal stem cells (hBMSCs) were isolated from bone marrow and characterized for the MSC phenotype (Delorme and Charbord, 2007). Cells were expanded in α -minimum essential medium (α -MEM; Sigma, St. Louis, MO, USA) with 10% fetal bovine serum (FBS; Biochrom AG, Germany), 1 ng/ml basic fibroblast growth factor (bFGF; PeproTech, USA) and 1% antibiotic/antimycotic mixture (Sigma). When a sufficient cell number was obtained, cells at passage 2 were seeded onto scaffolds at a density of 2.5×10^5 cells/scaffold. After 24 h of attachment, cell constructs were placed in new 24-well plates and 1 ml osteogenic medium containing dexamethasone 10^{-8} M (Sigma), ascorbic acid 50 $\mu\text{g/ml}$ (Sigma) and β -glycerophosphate 10 mM (Sigma) was added to each well. The cell constructs were cultured for 7, 14 and 21 days in a humidified atmosphere at 37°C containing 5% CO_2 .

2.3.1. Cell adhesion and morphology by scanning electron microscopy (SEM)

Cell adhesion, morphology and distribution throughout the scaffolds were analysed by SEM. Cell constructs were fixed and dehydrated using a sequence of ethanol gradients and further sputter-coated with gold (JEOL JFC-1100) for analysis, using a Leica Cambridge S360 SEM.

2.3.2. Cell viability assay – MTS test

Cell viability was assessed after 3 h, 7, 14 and 21 days using the MTS test. Cell constructs ($n = 3$) were washed in phosphate-buffered saline (PBS; Sigma), immersed in a mixture consisting of serum-free cell culture medium and MTS reagent in a 5:1 ratio and incubated for 3 h at 37°C in a humidified atmosphere containing 5% CO_2 .

Scaffolds alone, incubated for the same time in osteogenic medium, were used as controls. After this, 200 μl ($n = 3$) were transferred to 96-well plates and the optical density (OD) was measured on a microplate ELISA reader (BioTek, USA), using an absorbance of 490 nm.

2.3.3. Alkaline phosphatase (ALP) quantification

Samples were washed with phosphate buffered saline solution and transferred to 1.5 ml microtubes containing 1 ml ultra-pure water. Cell constructs ($n = 3$) were cryopreserved at -80°C for further analysis. Prior to ALP quantification, the samples were thawed and sonicated for 15 min.

Alkaline phosphatase (ALP) activity was measured by the specific conversion of *p*-nitrophenol phosphate (pNpp; Sigma) into *p*-nitrophenol (pNp). The enzymatic reaction was set up by mixing 100 μl of the sample with 300 μl of substrate buffer containing 1 M diethanolamine HCl, pH 9.8, and 2 mg/ml pNp. The solution was further incubated at 37°C for 1 h and the reaction was stopped by adding a solution containing 2 M NaOH and 0.2 mM EDTA. The OD was determined at 405 nm. A standard curve was made using pNp values in the range 0–20 $\mu\text{M/ml}$.

2.4. *In vivo* cranial defect in nude mice

Athymic nude mice, 7 weeks old (Harlan, Jerusalem, Israel) were used to examine the healing of cranial critical size bone defects in response to transplants in the defects according to the method described previously (Gupta *et al.*, 2008). All procedures involving the use of animals were conducted in accordance with the guidelines of the Institutional Animal Care and Use Committee of the Technion, Israel.

The *in vitro* cell constructs were cultured in osteogenic inducing medium for 2 weeks prior to implantation. Each scaffold was seeded with 1×10^6 cells. All surgery was performed under a protocol approved by the Animal Care and Use Committee of the Technion, Israel.

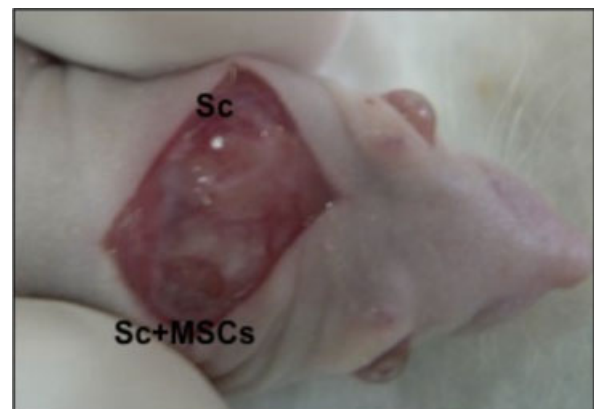


Figure 1. Low magnification image of cranial defects immediately after implantation. Cell constructs (Sc + MSCs) and scaffolds without cells (Sc)

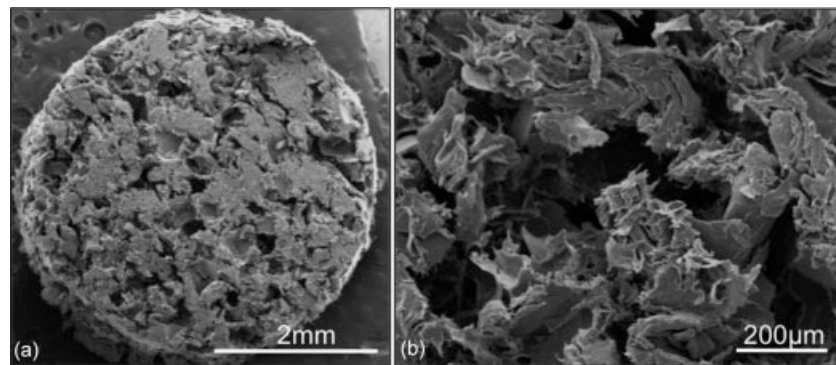


Figure 2. SEM micrographs of general view (a) and magnified view (b) of chitosan–PBS (50% wt) salt-leaching scaffolds

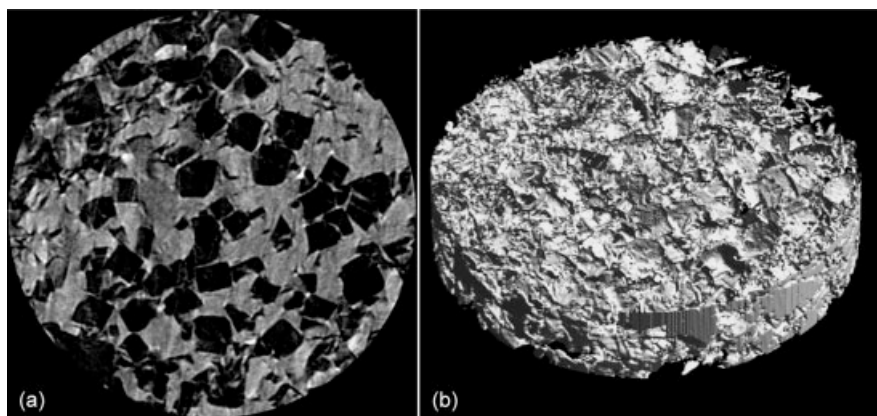


Figure 3. Representative 2D μ CT image (a) and 3D μ CT image (b) of the scaffold obtained from the sequence of 2D sections

Two bilateral critical-size circular defects (5 mm diameter \times 1 mm thick) were created using a hand drill and trephine bit in the parietal bones of the skull on either side of the sagittal suture line (Figure 1). Care was taken not to damage the sagittal suture or to interrupt the dura mater beneath the bone. During the procedure, sterile saline was dripped over the drilling site in order to avoid extensive heating and to protect the brain. Figure 1 illustrates the location of the defects in the mice crania. Surgery was performed under general anaesthesia (xylazine:ketamine, 1:1 solution in saline) by intraperitoneal injection.

Scaffolds were randomly implanted into the defects and divided into two experimental groups, which received the following implants: scaffolds seeded and cultured for 2 weeks with 1×10^6 hBMSC and scaffold without cells. A total of six nude mice were used and 12 cranial defects were created. Animals were kept under aseptic conditions. After 8 weeks post-surgery, animals were euthanized and crania were removed, cleaned and fixed immediately in formalin for 24 h, to be analysed by μ CT analysis. Briefly, the mice crania (with or without cells) were also analysed, using a high-resolution μ CT Skyscan 1072 scanner (Skyscan, Kontich, Belgium). Six specimens were scanned in high resolution mode, using a pixel size of $19.13 \mu\text{m}$ and an integration time of 1.7 ms. The X-ray source was set at 91 keV of energy and $110 \mu\text{A}$ of current. For all the scanned specimens, representative datasets of 1023 slices were transformed into binary, using a dynamic threshold of 255–120 to distinguish bone from polymeric material.

Table 1. Porosity, pore size and interconnectivity of chitosan-PBS scaffolds

Porosity (%)	Pore size (mm)	Interconnectivity (%)
59.0 ± 11.4	144.9 ± 33.4	60.9 ± 25.7

These data were used for morphometric analysis (CT Analyser v 1.5.1.5, SkyScan). 3D virtual models of the mice crania were created, visualized, and registered using image-processing software (ANT 3D Creator v 2.4, SkyScan).

2.5. Statistical analysis

The results of MTS and ALP are expressed as mean \pm standard deviation (SD), with $n = 3$ for each group. The statistical significance of differences was determined using the Student's *t*-test multiple comparison procedure at a confidence interval of 95% ($p < 0.01$).

3. Results and discussion

3.1. Characterization of scaffolds

SEM micrographs of the porous scaffolds are presented in Figure 2; Figure 2a shows the morphology of scaffolds 4 mm in diameter and 1 mm thick. Previous studies

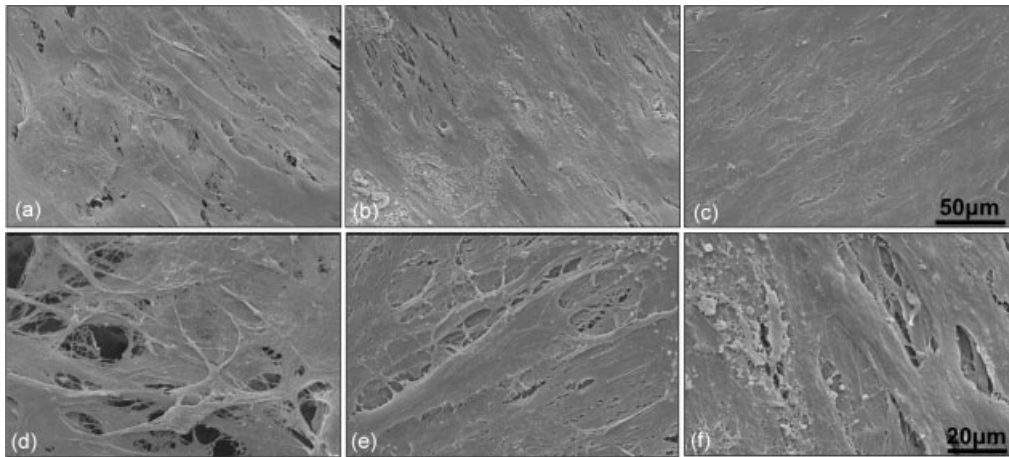


Figure 4. SEM micrographs of the cell-seeded scaffolds cultured under osteogenic induction, after 1 (a, b), 2 (c, d) and 3 (e, f) weeks

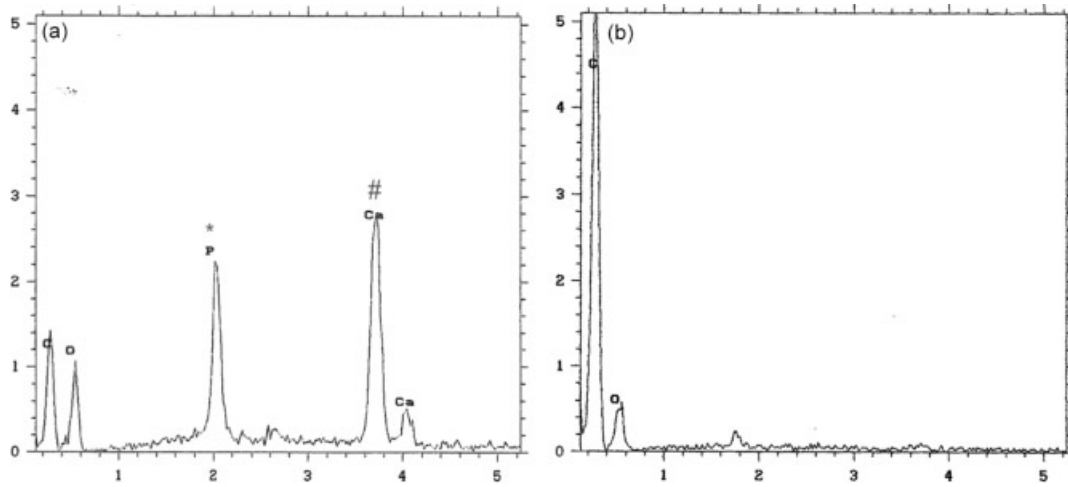


Figure 5. Energy dispersive spectra (EDS) showing the presence of calcium (#) and phosphorus (*) at the surface of the seeded chitosan–PBS (a) and scaffolds without cells (control) (b) after 3 weeks under osteogenic culture conditions

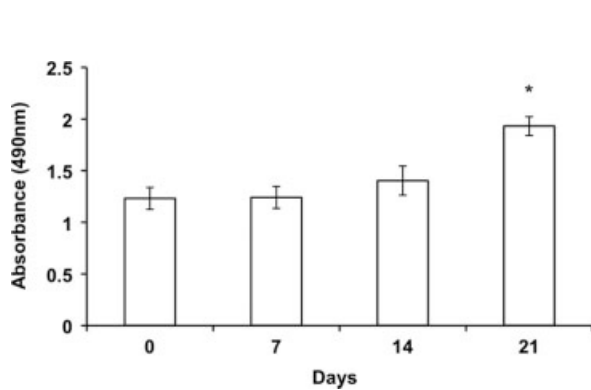


Figure 6. MTS viability assay of cell constructs and cultured chitosan–PBS scaffolds following 3 h (0 days), 7, 14 and 21 days after cell seeding. Results are expressed as mean \pm standard deviation (SD), with $n = 3$ for each bar. *Significant difference ($p < 0.01$) between testing conditions as a function of time

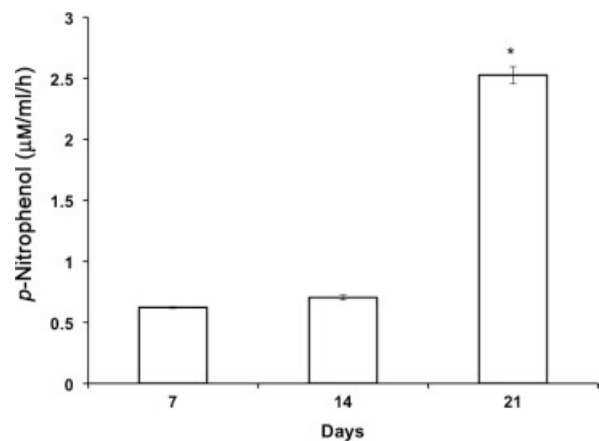


Figure 7. Alkaline phosphatase activity of hBMSCs cultured on the scaffolds after 1, 2 and 3 weeks under osteogenic induction. Results are expressed as mean \pm SD, with $n = 3$ for each bar. *Significant difference ($p < 0.01$) between conditions as a function of time

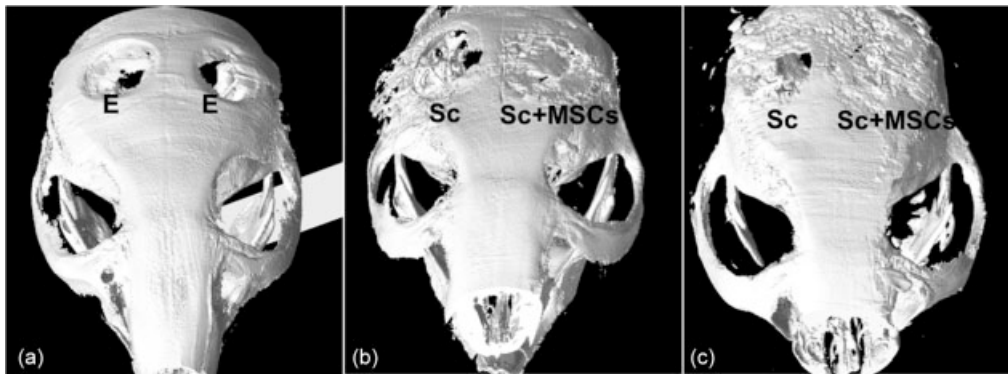


Figure 8. Micro-CT analysis of calvaria defects in nude mice. Images show the endpoint result, after 8 weeks, of bone healing upon implantation of scaffolds in the cranial defect of nude mice. E, empty; Sc, scaffold alone; Sc + MSCs, scaffolds with hBMSCs pre-cultured *in vitro* in osteogenic medium

(Alves da Silva *et al.*, 2010; Costa-Pinto *et al.*, 2008; Oliveira *et al.*, 2008) demonstrated that these scaffolds had adequate porosity (Figure 2b) to allow extensive cell proliferation.

For a detailed characterization of the scaffolds' internal structure, μ CT studies were conducted. Images of the region of interest were acquired and transformed into binary images (figure not shown). For all scaffolds, a dynamic threshold in the grayscale value range 255–150 was used to distinguish polymer material from pore voids. Individual two-dimensional (2D) analysis of the binary images (with a circle of interest of 4.5 mm²) was obtained from the scaffold cross-sections, consisting of 300 slices (Figure 3) and used for morphometric analysis (Table 1). The overall porosity of approximately 60% was consistent with the amount of leachable NaCl particles used in the preparation of the scaffolds. The average pore size was lower than expected, since the selected range of NaCl particles used was in the range 250–500 μ m. However, the mixing in the solid phase and the subsequent compression moulding may have caused significant reduction of the leachable particles, and consequently of the pore size. The level of interconnectivity indicated that most of the pores were open and probably allowed cell infiltration into the scaffolds' inner pores.

3.2. *In vitro* cell culture studies

3.2.1. Scanning electron microscopy (SEM)

SEM analysis showed that cells presented a great affinity to the scaffold surfaces, which was evident by the massive cell adhesion at the surface of the scaffolds (Figure 4). Previous results also showed this cell behaviour at the surface of similar scaffolds (Costa-Pinto *et al.*, 2009). After only 1 week of culture (Figure 4a, b), remarkable cell proliferation on the 3D structures was already visible. In the second week of culture a multilayer of cells covered the surfaces of the three-dimensional (3D) scaffold (Figure 4c, d). After 3 weeks of culture, it was visible that cell proliferation further developed into a dense multilayered cell structure (Figure 4e). Furthermore, there was

clear presence of Ca–P deposits (Figure 4f) corresponding to the produced mineralized ECM that was visible at higher magnifications. These results were confirmed by energy dispersive spectroscopy (EDS) analysis performed in samples cultured for up to 21 days (Figure 5). Unseeded scaffolds (kept immersed in osteogenic medium for the same period of time) were used as controls of EDS analysis. The presence of Ca and P peaks in the spectrum confirmed the presence of Ca and P elements at the surface of the cell-seeded scaffolds, which indicated that the cells were producing mineralized ECM and thus confirmed osteogenic differentiation after 21 days of culture.

3.2.2. Cell viability (MTS)

A cell viability assay (MTS) was used to assess the activity of the cells over time. The results demonstrated that hBMSCs seeded onto chitosan–PBS scaffolds were able to reduce the MTS substrate and progressively increased its metabolic activity during the time of culture (Figure 6). The obtained optical density values showed a significant increase after 21 days of culture. These results were corroborated by SEM images (Figure 4), with an increase of cell colonization over time. Furthermore, the presence of such active cells just after seeding (time 0) corresponded to a great seeding efficacy, which was due to the preference of the cells for these scaffolds instead of the tissue culture plate. These results were in accordance with previous results using different cells cultured onto similar scaffolds (Alves da Silva *et al.*, 2010; Costa-Pinto *et al.*, 2008, 2009; Oliveira *et al.*, 2008).

3.2.3. Alkaline phosphatase activity (ALP)

The ALP activity of human MSCs cultured onto the scaffolds did not follow the typical trend of this marker of osteogenic differentiation, as it was demonstrated after 21 days (Figure 7). After this time point, a significant increase in ALP activity was observed (Figure 7). Usually, ALP reaches a peak at an earlier time point. However, the presence of visible deposits of mineralized matrix after 21 days (SEM images, cell viability and EDS results)

suggested that the cells were viable and continued to deposit matrix, thereby indicating the cells' osteogenic differentiation.

3.3. In vivo cranial defect in nude mice

After the *in vitro* studies, the following step involved the *in vivo* validation, using a suitable animal model. For that, cell constructs were tested using a critical sized cranial defect. Briefly, we planned a study using the critical size calvaria bone defect in nude mice, using chitosan–PBS scaffolds and human cells. In this way, we were able to test both the viability of the 3D cell construct *in vivo* and the ability of those constructs to regenerate bone tissue. Cranial reconstruction represents a unique model to study bone regeneration, mainly because the calvaria is an anatomical area under limited mechanical stress, quite unlike the axial skeleton, which is subjected to long periods of compressive load (Mankani *et al.*, 2006). We used a 5 mm diameter defect, based on previous data found in the literature, showing that adult nude mice did not demonstrate significant calvaria bone healing in defects of 3, 4 and 5 mm diameter (Gupta *et al.*, 2008).

The scaffolds' diameter was optimized to enable some swelling before implantation. Previous studies have shown that these scaffolds have approximately 21% of water uptake. Based on these findings, we have implanted scaffolds 4.5 mm in diameter to match the size of the defect at the time of implantation.

Bone formation was evaluated by μ CT. This methodology is a low radiation and non-invasive method for studying the structure of bone samples. It can generate high-resolution images and provide accurate quantitative analysis of the bone structure parameters (Tuan and Hutmacher, 2005).

Bone possesses some self-healing capacity. However, there is a limit to the size of bone fractures and defects that can be self-repaired. This limit is designated the 'critical size defect' (An and Freidman, 1998; Wu *et al.*, 2010) and will not heal completely during the lifetime of the patient. For large bone defects, medical intervention is often necessary to repair the bone. In this study we have used hBMSCs cultured onto chitosan-based scaffolds in order to assess the ability of these tissue-engineered constructs to induce bone regeneration in nude mice cranial critical size defects. To our knowledge, there are few studies documenting the use of xenogeneic grafts (i.e. human cells and scaffolds) in the athymic nude mouse model (Cowan *et al.*, 2004; Dégano *et al.*, 2008; Kim *et al.*, 2006; Meinel *et al.*, 2005). We used nude mice in order to study the osteogenic potential of the hBMSCs seeded and cultured on chitosan–PBS scaffolds when implanted in a critical size defect. The μ CT results suggested that after 8 weeks of implantation, cell constructs promoted bone regeneration of the calvaria critical-size defect (Figure 8). The μ CT images also supported the enhanced bone ingrowth in

scaffolds cultured with MSCs. Some of the images clearly show an almost complete healing of the defect (Figure 8b, c). These findings are in accordance with previous results where scaffolds seeded with pre-induced osteogenic MSCs enhanced bone regeneration in critical size defect when the same animal model was used (Meinel *et al.*, 2005). Scaffolds *per se* were able to induce some bone regeneration/ingrowth (Figure 8c). New bone formation could be due to invading reparative cells from the dura or from adjacent host tissues. The selected implantation time seemed to be adequate for assessing the complete bone healing at the site defect, as shown in Figure 8c. Further studies need to be addressed using these scaffolds without cells, in immunocompetent animals, to confirm the tissue regeneration ability of chitosan–PBS scaffolds.

4. Conclusions

In the present study, chitosan–poly(butylene succinate) scaffolds were successfully produced by melt-based compression moulding followed by salt leaching. The microarchitecture of the scaffolds was assessed by SEM and μ CT, revealing a fully porous and interconnected 3D structure.

In vitro cell culture studies using hBMSCs have shown properties compatible with bone-engineering applications. The cells evidenced high levels of viability as a function of culture time and well correlated with SEM images that showed extensive cell colonization of the scaffolds. The produced ECM showed the presence of Ca and P elements, detected in EDS spectra of the cultured scaffold surfaces, which confirmed mineralization. Successful bone regeneration was achieved using critical size defects in the calvaria of nude mice, with prominent results for the *in vitro* cell construct compared to the scaffold without cells.

The combination of good biological performance of hBMSCs cultured onto chitosan-based scaffolds and the ability to regenerate bone tissue in a critical size defect significantly expands previous evidence that these materials can and will have a role to play in bone tissue-engineering strategies.

This study evidenced very positive results that highlight the possibility of chitosan–PBS–hBMSC constructs to be used as implants for non-load-bearing bone defects.

Acknowledgements

Ana Costa-Pinto was supported by Scholarship No. SFRH/24735/2005 from the Portuguese Research Council (Fundação para a Ciência e a Tecnologia; FCT). This work was partially supported by the EU Integrated Project GENOSTEM ('Adult mesenchymal stem cells engineering for connective tissue disorders: from the bench to the bedside'; Grant No. LSHB-CT-2003-5033161) and the European Network of Excellence EXPERTISSUES Project (Grant No. NMP3-CT-2004-500283).

References

- Alves da Silva M, Crawford A, Mundy J, *et al.* 2010; Chitosan/polyester-based scaffolds for cartilage tissue engineering: assessment of extracellular matrix formation. *Acta Biomater* **6**(3): 1149–1157.
- An Y, Freidman R. 1998; Animal Models in Orthopaedic Research. CRC Press: Boca Raton, FL, 1999; 241.
- Bianco P, Robey P. 2001; Stem cells in tissue engineering. *Nature* **414**(6589): 118–121.
- Castano-Izquierdo H, Alvarez-Barreto J, van den Dolder J, *et al.* 2007; Pre-culture period of mesenchymal stem cells in osteogenic media influences their *in vivo* bone forming potential. *J Biomed Mater Res A* **82**: 129–138.
- Correlo VM, Boesel LF, Bhattacharya M, *et al.* 2005; Properties of melt processed chitosan and aliphatic polyester blends. *Mater Sci Eng A* **403**(1–2): 57.
- Correlo VM, Boesel LF, Pinho E, *et al.* 2009; Melt-based compression-molded scaffolds from chitosan-polyester blends and composites: morphology and mechanical properties. *J Biomed Mater Res A* **91**(2): 489–504.
- Costa-Pinto AR, Correlo VM, Sol PC, *et al.* 2009; Osteogenic differentiation of human bone marrow mesenchymal stem cells seeded on melt based chitosan scaffolds for bone tissue engineering applications. *Biomacromolecules* **10**(8): 2067–2073.
- Costa-Pinto AR, Salgado AJ, Correlo VM, *et al.* 2008; Adhesion, proliferation, and osteogenic differentiation of a mouse mesenchymal stem cell line (BMC9) seeded on novel melt-based chitosan/polyester 3D porous scaffolds. *Tissue Eng A* **14**(6): 1049–1057.
- Cowan C, Shi Y, Aalami O, *et al.* 2004; Adipose-derived adult stromal cells heal critical-size mouse calvarial defects. *Nat Biotechnol* **22**(5): 560–567.
- Dégano I, Vilalta M, Bagó J, *et al.* 2008; Bioluminescence imaging of calvarial bone repair using bone marrow and adipose tissue-derived mesenchymal stem cells. *Biomaterials* **29**(4): 427–437.
- Delorme B, Charbord P. 2007; Culture and characterization of human bone marrow mesenchymal stem cells. *Methods Mol Med* **140**: 67–81.
- Di Martino A, Sittinger M, Risbud MV. 2005; Chitosan: a versatile biopolymer for orthopaedic tissue engineering. *Biomaterials* **26**(30): 5983–5990.
- Gimble J, Guilak F. 2003; Adipose-derived adult stem cells: isolation, characterization, and differentiation potential. *Cytotherapy* **5**(5): 362–369.
- Gomes M, Reis RL, Cunha AM, *et al.* 2001; Cytocompatibility and response of osteoblastic-like cells to starch-based polymers: effect of several additives and processing conditions. *Biomaterials* **22**(13): 1911–1917.
- Gupta D, Kwan M, Slater B, *et al.* 2008; Applications of an athymic nude mouse model of nonhealing critical-sized calvarial defects. *J Craniofac Surg* **19**: 192–197.
- Hipp J, Atala A. 2008; Sources of stem cells for regenerative medicine. *Stem Cell Rev* **4**: 3–11.
- Hutmacher D, Schantz J, Lam C, *et al.* 2007; State of the art and future directions of scaffold-based bone engineering from a biomaterials perspective. *J Tissue Eng Regen Med* **1**: 245–260.
- Kim Y, Bae Y, Suh K, Jung J. 2006; Quercetin, a flavonoid, inhibits proliferation and increases osteogenic differentiation in human adipose stromal cells. *Biochem Pharmacol* **72**(10): 1268–1278.
- Langer R, Vacanti J. 1993; Tissue engineering. *Science* **260**(5110): 920–926.
- Malafaya P, Pedro A, Peterbauer A, *et al.* 2005; Chitosan particles agglomerated scaffolds for cartilage and osteochondral tissue engineering approaches with adipose tissue derived stem cells. *J Mater Sci Mater Med* **16**: 1077–1085.
- Mankani M, Kuznetsov S, Wolfe R, *et al.* 2006; *In vivo* bone formation by human bone marrow stromal cells: reconstruction of the mouse calvarium and mandible. *Stem Cells* **24**: 2140–2149.
- Martins A, Alves C, Reis R, *et al.* 2009; Toward osteogenic differentiation of marrow stromal cells and *in vitro* production of mineralized extracellular matrix onto natural scaffolds. In *Biological Interactions on Materials Surfaces*, Puleo D, Bizios R (eds). Springer: New York.
- Martins AM, Santos MI, Azevedo HS, *et al.* 2008; Natural origin scaffolds with *in situ* pore forming capability for bone tissue engineering applications. *Acta Biomater* **4**(6): 1637–1645.
- Meinel L, Fajardo R, Hofmann S, *et al.* 2005; Silk implants for the healing of critical size bone defects. *Bone* **37**(5): 688–698.
- Montjovent M, Mathieu L, Schmoekel H, *et al.* 2007; Repair of critical size defects in the rat cranium using ceramic-reinforced PLA scaffolds obtained by supercritical gas foaming. *J Biomed Mater Res A* **83A**(1): 41–51.
- Oliveira JT, Correlo VM, Sol PC, *et al.* 2008; Assessment of the suitability of chitosan/polybutylene succinate scaffolds seeded with mouse mesenchymal progenitor cells for a cartilage tissue engineering approach. *Tissue Eng A* **14**(10): 1651–1661.
- Salgado A, Gomes M, Chou A, *et al.* 2002; Preliminary study on the adhesion and proliferation of human osteoblasts on starch-based scaffolds. *Mater Sci Eng C* **20**(2002): 27–33.
- Salgado AJ, Coutinho OP, Reis RL. 2004; Bone tissue engineering: state of the art and future trends. *Macromol Biosci* **4**(8): 743–765.
- Sarugaser R, Lickorish D, Baksh D, *et al.* 2005; Human umbilical cord perivascular (HUCPV) cells: a source of mesenchymal progenitors. *Stem Cells* **23**: 220–229.
- Schmitz J, Hollinger J. 1986; The critical size defect as an experimental model for craniomandibulofacial nonunions. *Clin Orthop Rel Res* **205**: 299–308.
- Tuan HS, Hutmacher DW. 2005; Application of micro-CT and computation modeling in bone tissue engineering. *Comput Aid Design* **37**(11): 1151–1161.
- Weissman I. 2000; Stem cells: units of development, units of regeneration, and units in evolution. *Cell* **100**(157–168).
- Wu X, Downes S, Watts DC. 2010; Evaluation of critical size defects of mouse calvarial bone: an organ culture study. *Microsc Res Techn* **73**(5): 540–547.
- Zarzycki R, Modrzejewska Z. 2003; [Use of chitosan in medicine and biomedical engineering]. *Polim Med* **33**(1–2): 47–58.